



HAL
open science

The anti-HIV pseudopeptide HB-19 binds the c-terminal end of nucleolin and prevents enchorage of virus particles on target cells.

S. Nisole, E.A. Said, C. Mische, M.C. Prevost, B. Krust, J. Blanco, Philippe Bouvet, J.P. Briand, A.G. Hovanessian

► To cite this version:

S. Nisole, E.A. Said, C. Mische, M.C. Prevost, B. Krust, et al.. The anti-HIV pseudopeptide HB-19 binds the c-terminal end of nucleolin and prevents enchorage of virus particles on target cells.. Journal of Biological Chemistry, 2002, 277, pp.20877-20886. 10.1074/jbc.M110024200 . hal-00023738

HAL Id: hal-00023738

<https://hal.science/hal-00023738>

Submitted on 31 May 2020

HAL is a multi-disciplinary open access archive for the deposit and dissemination of scientific research documents, whether they are published or not. The documents may come from teaching and research institutions in France or abroad, or from public or private research centers.

L'archive ouverte pluridisciplinaire **HAL**, est destinée au dépôt et à la diffusion de documents scientifiques de niveau recherche, publiés ou non, émanant des établissements d'enseignement et de recherche français ou étrangers, des laboratoires publics ou privés.

Copyright

The Anti-HIV Pentameric Pseudopeptide HB-19 Binds the C-terminal End of Nucleolin and Prevents Anchorage of Virus Particles in the Plasma Membrane of Target Cells*

Received for publication, October 17, 2001, and in revised form, March 26, 2002
Published, JBC Papers in Press, March 27, 2002, DOI 10.1074/jbc.M110024200

Sébastien Nisole^{‡§}, Elias A. Said[‡], Claudia Mische[‡], Marie-Christine Prevost[¶], Bernard Krust[‡],
Philippe Bouvet[¶], Alberto Bianco^{**}, Jean-Paul Briand^{**}, and Ara G. Hovanessian^{‡ ††}

From the [‡]Unité de Virologie et Immunologie Cellulaire (URA 1930 CNRS), [¶]Plateau Technique, Institut Pasteur, 28 Rue du Dr. Roux, 75724 Paris Cedex 15, [¶]Ecole Normale Supérieure de Lyon (CNRS-UMR 5665), 69007 Lyon, and ^{**}Institut de Biologie Moléculaire et Cellulaire, UPR 9021 CNRS, 15 Rue Descartes, 67084 Strasbourg Cedex, France

The multivalent pseudopeptide HB-19 that binds the cell-surface-expressed nucleolin is a potent inhibitor of human immunodeficiency virus (HIV) infection by blocking virus particle attachment and thus anchorage in the plasma membrane. We show that cross-linking of surface-bound HB-19A (like HB-19 but with a modified template) results in aggregation of HB-19A with surface nucleolin. Consistent with its specific action, HB-19A binding to different types of cells reaches saturation at concentrations that have been reported to result in inhibition of HIV infection. By using Chinese hamster ovary mutant cell lines, we confirm that the binding of HB-19A to surface nucleolin is independent of heparan and chondroitin sulfate proteoglycans. *In vitro* generated full-length nucleolin was found to bind HB-19A, whereas the N-terminal part containing the acidic amino acid stretches of nucleolin did not. The use of various deletion constructs of the C-terminal part of nucleolin then permitted the identification of the extreme C-terminal end of nucleolin, containing repeats of the amino acid motif, RGG, as the domain that binds HB-19A. Finally, a synthetic peptide corresponding to the last C-terminal 63 amino acids was able to inhibit HIV infection at the stage of HIV attachment to cells, thus suggesting that this domain could be functional in the HIV anchorage process.

HIV¹ infects target cells by the capacity of its envelope glycoproteins, the gp120-gp41 complex, to attach cells and induce the fusion of virus and cell membranes. The receptor complex

for HIV entry consists of the CD4 molecule and at least one of the members of the chemokine receptor family; CCR5 is the major coreceptor for macrophage-tropic HIV-1 isolates (R5), whereas that for T-lymphocyte-tropic isolates is CXCR4 (1). Although both CD4 and CXCR4/CCR5 are essential for the HIV entry process, the initial association of HIV particles to cells (referred to as attachment) could occur in the absence or blockade of these receptors (2–4). Accordingly, HIV attachment occurs efficiently in CD4⁺ human cells and even in heterologous cells albeit in the absence of membrane fusion and viral entry (4, 5). Several observations have pointed out that attachment of HIV particles to the cell surface seems to occur through the coordinated interactions on the one hand with heparan sulfate proteoglycans (2, 6, 7) and on the other hand with the cell-surface-expressed nucleolin (3, 4). Consequently, targeting any one of these components could result in the inhibition of HIV attachment. Indeed, HIV attachment could be blocked either by the fibroblast growth factor 2 that binds heparan sulfate proteoglycans or by the anti-HIV pseudopeptide HB-19 that binds nucleolin (3, 4). Contradictory hypothesis has been provided for the interaction of HIV particles with heparan sulfate proteoglycans. Saphire *et al.* (8) have reported that this interaction is mediated by cyclophilin A, *i.e.* a cellular protein that becomes incorporated into the viral membrane during HIV production, whereas Moulard *et al.* (9) have shown that the interaction is mediated by the basic residues in gp120.

The HB-19 pseudopeptide is a potent inhibitor of various T-lymphocyte- and R5-tropic HIV-1 isolates in CD4⁺ cell lines as well as in primary T-lymphocyte and macrophage cultures (1, 10, 11). HB-19 has no significant effect on the HIV-1 pseudotypes expressing glycoproteins of either Moloney murine leukemia virus or vesicular stomatitis virus, thus indicating that it is specific to the virus infection initiated by the HIV envelope glycoproteins (1, 3). The mechanism of the anti-HIV action of HB-19 is mediated through its capacity to bind cells specifically and to inhibit attachment of virus particles to CD4⁺ or CD4⁺ cells (1, 12, 13). At concentrations that inhibit attachment of HIV particles, HB-19 binds cells specifically and forms an irreversible complex with a cell-surface-expressed 95-kDa protein that we have identified as nucleolin (3, 4, 12). Recombinant preparations of HIV-1 gp120 bind partially purified preparations of nucleolin with a high affinity, comparable with that observed for the binding of gp120 to soluble CD4. Such binding is inhibited either by HB-19 or monoclonal antibodies against the V3 loop in gp120, thus suggesting that the interaction of HIV with nucleolin might occur through interactions implicating the V3 loop (3).

* This work was supported in part by grants from Institut Pasteur, and Ensemble Contre le SIDA, SIDACTION. The costs of publication of this article were defrayed in part by the payment of page charges. This article must therefore be hereby marked "advertisement" in accordance with 18 U.S.C. Section 1734 solely to indicate this fact.

§ Supported by a grant from the Ministère de l'Enseignement, de la Recherche et de la Technologie, France.

†† To whom correspondence should be addressed: Unité de Virologie et Immunologie Cellulaire, Institut Pasteur, 28 Rue du Dr. Roux, 75724 Paris Cedex 15, France. Tel.: 33-1-4568-8776; Fax: 33-1-4061-3012; E-mail: arahovan@pasteur.fr.

¹ The abbreviations used are: HIV, human immunodeficiency virus; HIV-1, HIV, type 1; AZT, azidothymidine; CHO cells, Chinese hamster ovary cells; FITC, fluorescein isothiocyanate; HB-19, 5(K_ψ(CH₂N)PR)TASP; HB-19A, 5(K_ψ(CH₂N)PR)TASP/αM in which the template was modified; gp120, external envelope glycoprotein of HIV-1; PFA, paraformaldehyde; R5, macrophage-tropic; TW70, a synthetic peptide specific to CXCR4; mAb, monoclonal antibody; PBS, phosphate-buffered saline; m.o.i., multiplicity of infection; FCS, fetal calf serum; LTR, long terminal repeat; RBD, RNA binding domain; GST, glutathione S-transferase.

Nucleolin is an RNA- and protein-binding protein that has been characterized in the literature mainly as a nucleolar protein (14, 15). However, several reports (16–20) have demonstrated that nucleolin is also expressed on the cell surface where it functions as a surface receptor for different ligands including the anti-HIV pseudopeptide HB-19 (3, 4, 21, 22). By studies using electron and confocal laser immunofluorescence microscopy, we have confirmed that nucleolin is expressed at the cell surface where it exists in close association with the intracellular actin cytoskeleton. Cell-surface expression of nucleolin is highly increased a few hours following stimulation of cell proliferation due to induction of nucleolin mRNA and protein synthesis. Interestingly, incubation of cells with a monoclonal antibody specific to nucleolin leads to the clustering of nucleolin at the external side of the plasma membrane as revealed by electron microscopy (20). Moreover, the anti-nucleolin antibody becomes internalized at 37 °C (20) consistent with other reports that surface nucleolin can mediate intracellular import of specific ligands (21, 22). The mechanism by which nucleolin is expressed on the cell surface still remains to be elucidated. It should be noted, however, that nucleolin is tightly associated with the cell surface, but it is readily solubilized by the non-ionic detergent Triton X-100 (20). Three main structural domains have been determined in nucleolin as follows: 1) the N-terminal domain containing several long stretches of acidic residues; 2) the central globular domain containing four RNA binding domains (RBDs); and 3) the extreme C-terminal domain containing nine repeats of the tripeptide motif arginine-glycine-glycine (RGG domain) (14, 15, 23).

Irreversible association of HIV particles in the plasma membrane of target cells, referred here as anchorage, requires at least the implication of heparan sulfate proteoglycans, surface-expressed nucleolin, the CD4 receptor, and one of the members of the chemokine receptor family. Interestingly, despite the attachment of HIV to cells of different species not expressing CD4, anchorage of virus particles does not occur in CD4⁻ cells. Anchorage of virus particles on CD4⁺ cells can be prevented in the presence of neutralizing anti-V3 loop or anti-CD4 antibodies or treatment of cells with HB-19. Here we have used a new generation of the HB-19 pseudopeptide 5(K)₄(CH₂N)PR)-TASP (10) (referred here as HB19A) which, like HB-19, presents pentavalently the K)₄(CH₂N)PR moiety but coupled to a modified TASP template. HB-19A has anti-HIV properties identical to HB-19. Consistent with our previous results obtained with HB-19 (4), we show that HB-19A binds the cell-surface-expressed nucleolin independent of the expression of cell-surface heparan and chondroitin sulfate proteoglycans. Furthermore, cross-linking of surface-bound HB-19A results in capping of surface nucleolin and its colocalization with the pseudopeptide. By using deletion constructs of nucleolin, the C-terminal tail of nucleolin containing the nine repeats of the RGG motif was identified as the HB-19A-binding site. Moreover, this domain in nucleolin inhibited HIV-1 infection in a dose-dependent manner by preventing attachment of virus particles to cells. Our results confirm that nucleolin is the target of the anti-HIV pseudopeptide HB-19A and point out that the RGG domain provides a model for the development of novel inhibitors of HIV infection.

EXPERIMENTAL PROCEDURES

Materials—The monoclonal antibody (mAb) D3 specific for human nucleolin was provided by Dr. J. S. Deng (24). Rabbit antiserum raised against a purified preparation of hamster nucleolin was provided by Dr. M. Erard. mAb CBT4 reacting with the gp120-binding site in human CD4 (5) was provided by Dr. Eugene Bosmans (clone CB-T4-2). mAb N11/20 directed against the V3 loop of HIV-1 LAI isolate was provided by Dr. J. C. Mazie. mAb 110-4 against HIV-1 LAI V3 loop was

the generous gift of the Genetic Systems. mAb HB10 AB2A against CD45 was provided by Dr. R. Siraganian. HIV-1 neutralizing serum 1 and serum 2 and control human IgG were obtained from Dr. L. Vujcic through the AIDS Research and Reference Reagent Program, AIDS Program, NIAID, National Institutes of Health. Rabbit anti-biotin concentrate (IgG fraction) was obtained from Enzo Diagnostics, Inc., New York. FITC-conjugated goat anti-mouse IgG was purchased from Sigma. FITC-conjugated F(ab')₂ fragment rabbit anti-human Ig and Texas Red dye-conjugated donkey anti-rabbit IgG were from Jackson ImmunoResearch Laboratories. Texas Red dye-conjugated goat anti-human IgG was from Vector Laboratories. Goat anti-rabbit antibodies coupled to gold beads of 10 nm in diameter and goat anti-human antibodies coupled to gold beads of 15 nm in diameter were obtained from Amersham Biosciences.

Peptide Constructs—In these experiments a new generation of the HB-19 pseudopeptide 5(K)₄(CH₂N)PR)-TASP (10) was used in which the template is made of four lysine residues linked by their ε-NH₂ groups with an alanine residue introduced as a spacer at the C terminus (1). The five K)₄(CH₂N)PR moieties were then assembled on the α-amino groups of the four lysine residues and on the ε-amino group of the N-terminal lysine residue. This anti-HIV pseudopeptide with the modified TASP template is referred here as HB-19A. The synthesis of HB-19A was performed according to the protocol described previously (1) until the introduction of the N-terminal Lys of the K)₄(CH₂N)PR motif. The reduced amide bond between Lys and Pro was formed on the resin by reductive amination of the nitrogen-protected aminoaldehyde *t*-butoxycarbonyl-Lys(*t*-butoxycarbonyl)-CHO (2.5-fold excess, twice) in dimethylformamide containing 1% acetic acid along 1 h (10). For the synthesis of the biotinylated HB-19A, the biotin moiety was coupled after the C-terminal Ala using a *N*-(9-fluorenyl)methoxycarbonyl (Fmoc)-Lys(biotin)-OH derivative. A 6-aminohexanoic acid was introduced as a spacer between Lys(biotin) residue and the polylysine template (1). The anti-HIV cyclic peptide TW70 specific for CXCR4 was synthesized as described (25, 26). The TW70 peptide has the amino acid sequence RRWCYRK₇KPYRKCR; the ₇K has been introduced in the sequence of this peptide to stabilize the β-turn in the final structure. The synthetic peptide corresponding to the last 63 amino acid residues at the C-terminal tail of human nucleolin had the following sequence, amino acids ⁶⁴⁸KGEGGFGGRRGGGGFGGRRGGRRGGFGGRRGGFGGRRGGFGGRRGGFGGRRGGGGDDHKPQGGKTKFE⁷⁰⁷. All peptides were obtained at a high purity (>95%), and their integrity was controlled by matrix-associated laser desorption/ionization-time-of-flight analysis (27). HB-19A was iodinated (5 × 10³ μCi/μmol) using the Bolton-Hunter reagent (PerkinElmer Life Sciences) by a procedure as recommended by the manufacturer.

Cell Lines and Virus Preparations—CEM (clone 13) and MT-4 T-lymphocyte human cell lines were propagated in RPMI 1640 (BioWhittaker, Verviers, Belgium). Human HeLa cells were cultured in Dulbecco's modified Eagle's medium (Invitrogen). Human HeLa-CD4-LTR-*lacZ* expressing or not expressing CCR5 were referred to as HeLa P4-C5 and HeLa P4, respectively. These HeLa cells (provided by Drs. P. Charneau and O. Schwartz; Institut Pasteur, Paris, France) were cultured in Dulbecco's modified Eagle's medium (Invitrogen) supplemented with G418 sulfate (500 μg/ml) for the HeLa P4 cells and with G418 sulfate (500 μg/ml)/hygromycin B (300 μg/ml) (Calbiochem-Novabiochem) for the HeLa P4-C5 cells (1). Chinese hamster ovary cell lines were obtained from American Type Culture Collection: wild type cells (CHO K1) and mutant cells defective in heparan sulfate proteoglycan expression (CHO 677) or heparan and chondroitin sulfate proteoglycan expression (CHO 618) (28, 29). CHO cell lines were cultured in Ham's F12K medium. All cells were cultured with 10% (v/v) heat-inactivated (56 °C, 30 min) fetal calf serum (FCS; Roche Molecular Biochemicals) and 50 IU/ml penicillin-streptomycin (Invitrogen). The HIV-1 LAI isolate was propagated and purified as described previously (1, 13). The HIV-1 Ba-L isolate (30) was provided by the AIDS Program, NIAID, National Institutes of Health. The m.o.i. of the HIV-1 for different infections was 1. For the assay of HIV-1 LAI attachment, anchorage and colocalization studies purified virus was used at an m.o.i. of 3.

Assay of HIV Infection in HeLa CD4⁺ Cells—HIV-1 LAI infection was monitored indirectly in HeLa-CD4-LTR-*lacZ* cells (HeLa P4 cells) containing the bacterial *lacZ* gene under the control of HIV-1 LTR. HIV-1 entry and replication result in the activation of the HIV-1 LTR leading to the expression of β-galactosidase. At 48 h post-infection, cells were lysed and assayed for β-galactosidase activity using the chlorophenol red β-D-galactopyranoside as a substrate. The absorbance was measured at 570 nm (1). The HIV-1 Ba-L infection was monitored in HeLa-CD4-LTR-*lacZ* cells also expressing CCR5 (HeLa P4-C5 cells) as above (1).

Assay of HIV Particle Attachment and Entry—The attachment assay was carried out at room temperature (20 °C) for 1 h to block viral entry (31) and potential HIV endocytosis (32). Cells were then washed extensively with culture medium containing 10% FCS to eliminate unbound HIV particles, and the amount of p24 associated with cells was measured in nucleus-free cell extracts as an estimate for the amount of HIV attached to cells by p24 Core Profile enzyme-linked immunosorbent assay (PerkinElmer Life Sciences) (5, 31). To demonstrate that most of the p24 associated with cells represented HIV particles bound on the surface of cells, samples of cells incubated with virus were washed with PBS (containing 1 mM EDTA) before treatment with trypsin to eliminate virus bound on the cell surface as described before (1). Evidence that the virus attachment was mediated by the HIV envelope glycoprotein gp120 was provided by the capacity of anti-V3 loop mAbs N11/20 or 110/4 to inhibit the attachment process (5).

Confocal Microscopy—For the colocalization experiments, MT4 cells in RPMI medium containing 10% FCS were incubated in the absence or presence of HIV (m.o.i. 3) and the biotin-coupled HB-19A (1 μ M) for 30 min, before washing with RPMI medium containing 1% FCS. Cells were then further incubated for 60 min in the presence of either anti-HIV serum (1/50) or rabbit anti-biotin serum (1/100) to cross-link virus particles and HB-19A adsorbed on the cell surface, respectively. Cells were first washed in RPMI, 1% FCS and second with PBS before fixation with 0.25% PFA. Such partially fixed cells were incubated (20 °C, 45 min) with mAb D3 specific to nucleolin or to mAb HB10 specific to CD45 (10 μ g/ml). After washing, cells were fixed with 3.7% PFA and washed again, and the primary antibodies were revealed by the addition of either goat Texas Red dye-conjugated anti-human antibodies, donkey Texas Red dye-conjugated anti-rabbit antibodies, or goat FITC-conjugated anti-mouse IgG. Finally, cells were added in 8-well glass slides (LAB-TEK Brand, Nalge Nunc International, Naperville, IL) that were precoated with poly-L-lysine at 30 μ g/ml (Sigma) and left for 15 min before washing the attached cells with PBS and proceeding for laser scanning confocal immunofluorescence microscopy (Leica TCS4D) (20).

Anchorage of HIV Particles on Target Cells—HeLa and HeLa P4 cells were plated 24 h before the experiment in 8-well glass slides. Cells were then incubated in fresh culture medium in the absence or presence of different reagents for 30 min at 37 °C before addition of HIV-1 and further incubation at room temperature for 1 h. Cell monolayers were then washed with PBS to eliminate unbound HIV particles before incubation in medium containing 1% FCS and the anti-gp120 mAb 110-4 (20 μ g/ml) for 1 h at room temperature to reveal HIV gp120 on the surface of HIV particles still remaining accessible after virus attachment. Cells were then fixed with 3.7% PFA before addition of goat FITC-labeled anti-mouse antibodies and processed for confocal microscopy (13). Under these experimental conditions the staining was observed only on the cell surface.

Electron Microscopy—MT4 cells in RPMI at 10% FCS were incubated (30 min at 37 °C) with HIV-1 LAI at an m.o.i. of 3. Cells were then washed with RPMI at 1% FCS and incubated (60 min, 20 °C) with anti-HIV-1 human serum (1/50) to cross-link HIV particles bound on the surface of cells. After washing in culture medium, cells were washed in PBS and partially fixed with 0.25% PFA for 10 min at 20 °C. After an extensive wash in PBS, cells were incubated (45 min, 20 °C) with the biotin-conjugated mAb D3 against nucleolin (10 μ g/ml). Cells washed in PBS were then fixed with 3.5% PFA before addition of rabbit anti-biotin antibodies (1/100) and incubation for 45 min at 20 °C. These rabbit antibodies were revealed by goat anti-rabbit antibodies (IgG) coupled to gold beads of 10 nm in diameter, whereas human antibodies were revealed by goat anti-human antibodies (IgG) coupled to gold particles of 15 nm in diameter (1/25). Finally, cells were washed in PBS and fixed (overnight, 4 °C) in 1.6% glutaraldehyde. After further washing in PBS, cells were post-fixed with osmium tetroxide, dehydrated in ethanol, and embedded in Epon. Sections were collected on Formvar carbon-coated grids, stained with uranyl acetate and lead citrate, and observed using an electron microscope (Jöel 1200EX).

Assay of HB-19A Binding to Cells—Cells were plated at 10^4 cells/well in 96-well plates for the 125 I-labeled HB-19A binding or at 10^5 cells/well in 24-well plates for the biotinylated HB-19A binding. Twenty four hours later, binding experiments were performed after incubation of the cell monolayers in fresh culture medium for 1 h at room temperature (about 21 °C) to cool cells. It should be noted that intracellular entry of HB-19A is inhibited more than 90% at room temperature. Cells were incubated (30 min at room temperature) with different concentrations of the 125 I-labeled HB-19A or the biotinylated HB-19A before washing cells in culture medium containing 10% FCS. For total amount of binding (specific and nonspecific), cells were washed 7 times with cul-

ture medium. For specific binding measurements, cells were first washed 3 times in culture medium supplemented with 150 mM NaCl thus bringing the final concentration of NaCl to 300 mM followed by 4 washings in culture medium. Washed cells were processed to reveal either the 125 I-labeled HB-19A or the biotinylated HB-19A. For the 125 I-labeled HB-19A binding, cell monolayers were extracted in 1% SDS, and the radioactivity was measured in an automatic gamma counter (LKB Wallac Clini Gamma 1272). For the biotinylated HB-19A, cells were first incubated (30 min, 6 °C) in medium containing streptavidin-horseradish peroxidase conjugate (Amersham Biosciences) before washing twice with medium followed by two washes in PBS containing bovine serum albumin (1%). Cell monolayers were extracted in 400 μ l of lysis buffer E (20 mM Tris-HCl, pH 7.6, 150 mM NaCl, 5 mM MgCl₂, 0.2 mM phenylmethylsulfonyl fluoride, 5 mM β -mercaptoethanol, aprotinin (1000 units/ml), and 0.5% Triton X-100) and the nucleus-free extracts were centrifuged at 12,000 \times g for 10 min. Finally, *ortho*-phenylenediamine solution was added in the dark, and the absorbance was measured at 405 nm.

Purification of Cell Surface-associated Nucleolin—These experimental conditions were optimized previously for samples from CEM and HeLa cells (3, 4). Briefly, CHO cell monolayers in 150-cm² flasks (about 25×10^6 cells/flask) were incubated in 10 ml of culture medium (Ham's F12K medium with 10% fetal calf serum) containing the biotinylated HB-19A (5 μ M) for 45 min at 6 °C. After washing extensively in PBS containing 1 mM EDTA (PBS/EDTA), nucleus-free cell extracts were prepared in lysis buffer E containing unlabeled HB-19A (50 μ M). The complex formed between cell-surface-expressed nucleolin and the biotinylated HB-19A was isolated by purification of the extracts using avidin-agarose (100 μ l; ImmunoPure Immobilized Avidin from Pierce) in PBS/EDTA. After 2 h of incubation at 4 °C, the samples were washed extensively with PBS/EDTA. The purified proteins were denatured by heating in the electrophoresis sample buffer containing SDS and analyzed by SDS-PAGE. The presence of nucleolin was then revealed by immunoblotting using rabbit polyclonal antibodies against hamster nucleolin.

Immunoblotting—Samples were separated on a 10% SDS-PAGE. After electrophoresis, proteins were transferred to a 0.22-mm polyvinylidene difluoride sheet (Bio-Rad). The electrophoretic blots were saturated with casein-based blocking buffer (Genosys) and washed extensively before incubation with rabbit polyclonal antibodies against hamster nucleolin. After extensive washing, the filter was treated with horseradish peroxidase-conjugated rabbit anti-mouse immunoglobulin (Amersham Biosciences). The reacting bands were visualized with an enhanced chemiluminescence (ECL) reagent and by exposure to autoradiography film (Amersham Biosciences).

Generation of Deletion Constructs of Human Nucleolin—The pcDNA4 Nuc, pcDNA4 NucN, and pcDNA4 NucC plasmids encode the full-length human nucleolin open reading frame, its N-terminal part (corresponding to the first 275 amino-acids) and its C-terminal part (corresponding to the last 433 amino-acids), respectively. The full-length human nucleolin and its truncated derivatives were generated by PCR using high fidelity DNA polymerase (Expand High Fidelity PCR System, Roche Molecular Biochemicals) and the following oligonucleotides: NucN-F/NucC-R for Nuc, NucN-F/NucN-R for NucN, and NucC-F/NucC-R for NucC. The following oligonucleotides were used: NucN-F, 5'-GGGGATCCATGGTGAAGCTCGCGAAGGCAGG-3'; NucN-R, 5'-CCGAATCTTCTTTGACAGGCTCTCCTCCT-3'; NucC-F, 5'-GGGGATCCGAAGCACCTGGAAAACGAAAG-3'; NucC-R, 5'-GGGAATTCCTATCAAACTTCGCTTCTTTCCTTG-3'. The PCR products, containing *Bam*HI and *Eco*RI restriction sites (underlined), were digested by the corresponding restriction enzymes and inserted between *Bam*HI and *Eco*RI sites of the pcDNA4His/Max C plasmid (Invitrogen).

Deletion constructs of the C-terminal half of human nucleolin were generated by PCR using human nucleolin cDNA as template. R1234G (1234 corresponding to the four RNA Binding Domains and G to the Gly/Arg-rich RGG domain) encodes the full-length C-terminal part of nucleolin and was amplified with R1N and RGGC primers. The other constructs encode the same part, deleted from one or more domains as follows: R1234 (R1N/R4C), R12 (R1N/R2C), R123 (R1N/R3C), R234 (R2N/R4C), R234G (R2N/RGGC), R34 (R3N/R4C), R34G (R3N/RGGC), and RGG (RGGN/RGGC), using the primer pairs indicated in parentheses. The sequences of oligonucleotides are as follow: R1N, 5'-GGA-TCCAATCTCTTTGTTGGAAACCTAAAC-3'; R2N, 5'-GGATCCACAC-TTTTGCTAAAATCTCCCT-3'; R2C, 5'-GAATCTCTTTGATTCACC-CTCCAAGTGCT-3'; R3N, 5'-GGATCCACTCTGGTGTGTTAAACCACT-CTCCT-3'; R3C, 5'-GAATCTTTGGATGGCTGGTCTTGGCATT-3'; R4N, 5'-GGATCCACTCTGTTTGTCAAAGGCCTGTCT-3'; R4C, 5'-GA-ATTCAGGTTTGGCCAGTCCAAGGTAAC-3'; RGGN, 5'-GGATCCA-

AGGGTGAAGGTGGCTTCGGGGGT-3'; and RGGC, 5'-GAATTCCTA-TTCAAACCTCGTCTTCTTCC-3'. PCR products were subcloned in pCR2.1 TOPO plasmid (Invitrogen) by T/A cloning, removed using *Bam*HI and a *Eco*RI sites inserted at their 5'- and 3'-ends, respectively (underlined), and cloned between the corresponding sites of pGEX-N3 plasmid (Amersham Biosciences), in-frame to glutathione *S*-transferase (GST).

In Vitro Transcription and Translation of Human Nucleolin—The TNT-coupled reticulocyte lysate system (Promega) was used to produce the wild type nucleolin (pcDNA4 Nuc) and the N- and C-terminal parts of nucleolin (pcDNA4 NucN and pcDNA4 NucC containing amino acids 1–308 and 309–707) by *in vitro* transcription/translation. Reactions were performed by using 2 μ g of each plasmid and 20 μ Ci of [³⁵S]methionine/cysteine (ProMix; Amersham Biosciences) per 50 μ l of TNT reticulocyte lysate, as specified by the manufacturer.

To assay the HB-19A binding capacity of the generated nucleolin and nucleolin truncated constructs, 25 μ l of translation products were diluted in 25 μ l of modified BI buffer (20 mM Tris-HCl, pH 7.6, 100 mM NaCl, 50 mM KCl, 2 mM EDTA, 2% Triton X-100, 1000 units/ml aprotinin), centrifuged at 12,000 \times *g* for 10 min at 4 °C, and diluted in 150 μ l of PBS. Binding reactions were performed by incubating 200 μ l of each diluted lysates with the biotinylated HB-19A for 1 h at 4 °C. Complexes formed between nucleolin deletion constructs and biotinylated HB-19A were isolated by purification of the extracts using avidin-agarose (100 μ l) in PBS/EDTA (12). After 2 h of incubation at 4 °C, the samples were washed extensively with PBS/EDTA. The purified proteins were eluted by heating in the electrophoresis sample buffer containing SDS and analyzed by SDS-PAGE. The [³⁵S]methionine/cysteine-labeled proteins were revealed by fluorography.

Expression and Purification of Recombinant Nucleolin Constructs—*Escherichia coli* BL21(DE3) cells were transformed with each pGEX-N3 plasmid coding for truncated derivatives of the C-terminal part of human nucleolin. Cells were grown overnight at 37 °C in 100 ml of Terrific Broth containing 100 μ g of ampicillin per ml. After 1:50 dilution in 100 ml of fresh medium, cells were grown at 30 °C to a 600 nm absorbance of ~0.5 (6 h) and induced with 0.5 mM isopropyl-1-thio-D-galactopyranoside for an additional 2 h. Bacteria were pelleted at 4,000 \times *g* for 10 min at 4 °C, resuspended in 5 ml of PBS containing 0.2 mM phenylmethylsulfonyl fluoride and 1 mM dithiothreitol, and frozen at –20 °C overnight. After being thawed on ice, the bacterial suspensions were frozen again in a dry ice-methanol bath, thawed on ice, sonicated three times for 30 s each time on ice, adjusted to 1% (w/v) with Triton X-100, and centrifuged at 9,000 \times *g* for 20 min at 4 °C. The presence of proteins in cell extracts was monitored by SDS-PAGE with Coomassie Blue staining, and their respective concentrations were estimated and adjusted.

To assay HB-19A binding capacity, bacterial extracts were first diluted 5-fold in PBS/EDTA before centrifugation at 12,000 \times *g* for 10 min at 4 °C. Supernatants were then incubated for 1 h at 4 °C with the biotinylated HB-19A, and the complexes were recovered on avidin-agarose (100 μ l) in PBS/EDTA by incubation for 2 h at 4 °C. The samples were washed 3 times with PBS/EDTA and twice with PBS/EDTA containing additional 150 mM NaCl (resulting to a final concentration of 300 mM NaCl) to eliminate unbound material and also the non-specifically bound proteins. The purified proteins were eluted by heating in the electrophoresis sample buffer containing SDS and analyzed by immunoblotting using anti-GST monoclonal antibody B-14 (Santa Cruz Biotechnology, Inc.).

Purification of the GST Fusion Proteins—The truncated nucleolin constructs R1234G and R1234 were purified directly from bacterial lysates using glutathione-Sepharose 4B affinity chromatography (Amersham Biosciences) by a procedure as recommended by the manufacturer. The proteins were recovered in the glutathione elution buffer. The purified proteins were dialyzed against PBS and stored at –80 °C.

RESULTS

Several Components Are Required for Anchorage of HIV Particles in the Plasma Membrane—The stable (*i.e.* functional) association of HIV particles with the plasma membrane of target cells, referred to as “anchorage,” can be monitored by inducing the cross-linking of adsorbed virions with anti-gp120 antibodies. Indeed, when particles are bound on the surface of CD4⁺-permissive cells, the antibody-induced cross-linking leads to their aggregation at one pole of the cell. This antibody-dependent cross-linking of HIV particles on CD4⁺ cells permits monitoring the anchorage of virus particles in the plasma mem-

brane by confocal laser immunofluorescence microscopy. The fluorescent signal of HIV is found only at the cell membrane, because it disappears when scanning is performed at an intracellular level (13). In contrast, although HIV particles are able to attach to CD4-negative cells, cross-linking with anti-HIV antibodies washes out particles, thus confirming that attachment alone is not sufficient for anchorage of virions (not shown). Besides the requirement of CD4, the proper anchorage of HIV particles on target cells is coordinated by several surface components, including heparan sulfate proteoglycans, nucleolin, and chemokine receptors. Consequently, anchorage is inhibited either by neutralizing anti-CD4 antibodies, the fibroblast growth factor 2 which binds heparan sulfate proteoglycans, the pseudopeptides HB-19 or HB-19A which bind nucleolin, and the TW70 peptide which binds CXCR4 (Refs. 1, 4, 13, and 26 and data not shown).

HB-19A-induced Capping of Surface Nucleolin—By using the biotinylated HB-19, we have shown previously (3, 4, 12) that HB-19 binds specifically the cell-surface-expressed nucleolin and forms an irreversible complex with it. The nucleolin-HB-19 complex then becomes internalized at 37 °C but not at reduced temperatures (33). Indeed at 20 °C, HB-19 remains attached to the cell surface without entering the cytoplasm. Similarly, internalization of the anti-nucleolin antibody is also blocked at reduced temperatures thus suggesting that internalization via nucleolin occurs by an active process (20). For these reasons, cell binding experiments with HB-19A carried out here were performed at 20 °C.

In general, the cross-linking of a ligand leads to the clustering or capping of its surface receptor. Accordingly, we investigated distribution of surface nucleolin following the cross-linking of the biotinylated HB-19A using anti-biotin antibodies. The biotinylated HB-19A binding to MT4 cells was carried out for a short period at 20 °C before washing cells and further incubation with anti-biotin antibodies to induce lateral aggregation of HB-19A. Cells were then partially fixed with 0.25% PFA before adding the monoclonal antibody against nucleolin to reveal the steady state distribution of nucleolin at the plasma membrane. Under such experimental conditions, the nucleolin signal was patched at one pole of the cell, which coincided with the HB-19A signal (Fig. 1A). On the other hand, in control cells incubated without HB-19A the nucleolin signal was detected as evenly distributed in the plasma membrane and in a diffused state (Fig. 1B). The ligand-dependent capping of surface nucleolin observed in the presence of HB-19A appeared to be a specific event because the distribution of another surface protein CD45 was affected only slightly. In control cells, the CD45 signal was found to be more or less evenly distributed at the periphery of cells, and when HB-19A was aggregated at distinct spots, the distribution of CD45 still remained somewhat around the cell periphery, although more condensed signals at positions when the HB-19A spots were observed (Fig. 1C). This latter was most probably due to patching of membrane components (34) at positions where HB-19A was aggregated. Interestingly, capping of surface nucleolin was also observed in cells following cross-linking of HIV particles bound to cells, and consequently the HIV signal became colocalized with that of nucleolin (Fig. 1D). Under such experimental conditions HIV particles also cause capping of CD4 and CXCR4 but not CD45 (34). It should be noted that the binding of the parental HB-19 to surface nucleolin is prevented by preincubation of cells with HIV particles thus suggesting the existence of a competition between HIV and HB-19 to bind surface nucleolin (4). This and the capacity of HB-19A and HIV to cluster surface nucleolin are consistent with the nucleolin being a common target for both ligands.

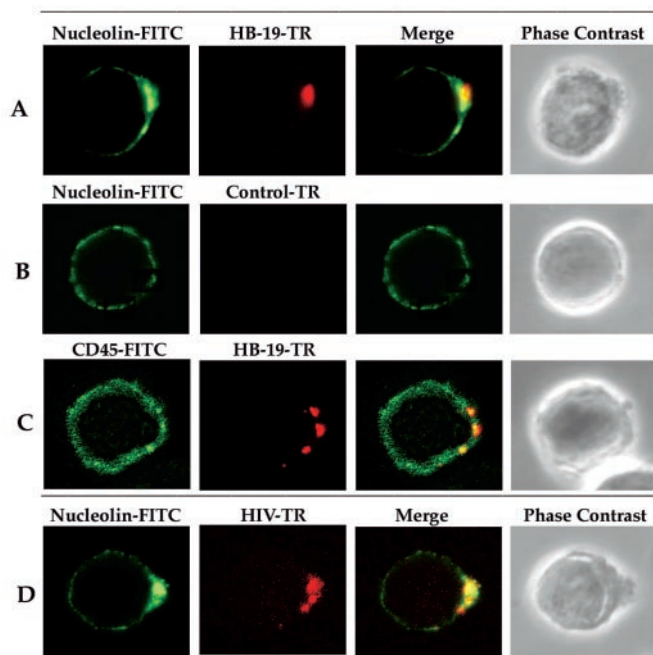


FIG. 1. Cross-linking of surface-bound HB-19A or HIV particles results in capping of surface nucleolin. A–C, MT4 cells were incubated with the biotinylated HB-19A at 20 °C for 30 min before further incubation (20 °C for 60 min) in the presence of rabbit anti-biotin antibodies (*panels HB-19A-TR*) to induce patching of surface-bound HB-19A. After partial fixation, the coaggregation of HB-19A with nucleolin (A and B) and CD45 (C) was investigated using murine mAbs against nucleolin and CD45. B, the experiment was as in A but in the absence of HB-19A. D, MT4 cells were incubated (37 °C, 30 min) with HIV-1 LAI before washing and further incubation (20 °C for 60 min) in the presence of anti-HIV human serum to induce aggregation of virus particles bound to cells (34). After partial fixation, the coaggregation of HIV with nucleolin was investigated by using the anti-nucleolin mAb. Bound rabbit antibodies were revealed by donkey Texas Red dye (TR)-conjugated anti-rabbit antibodies, and human antibodies were revealed by goat Texas Red dye-conjugated anti-human antibodies, whereas murine mAbs were revealed by goat FITC-conjugated anti-mouse IgG. A cross-section for each staining is shown with the merge of the two colors and the respective phase contrast. Experimental conditions are described under “Experimental Procedures.”

By electron microscopy, we have demonstrated previously (20) that when surface nucleolin is cross-linked by the anti-nucleolin antibody, it becomes clustered at the external side of the plasma membrane. Here we show that in MT4 cells with anchored HIV, surface nucleolin also becomes abundant at a region in close contact with HIV particles (Fig. 2A). This is revealed by the presence of several gold particles of 10 nm in diameter corresponding to the anti-nucleolin antibody. In some cases, we were able to colocalize the nucleolin signal with that of the gp120 on the HIV particle. An example is shown in Fig. 2B showing a 15 nm gold particle corresponding to the anti-gp120 antibody surrounded by four 10 nm gold particles corresponding to the anti-nucleolin antibody. The detection of gp120 on the surface of HIV particles was dependent on its association with the plasma membrane (Fig. 2B). This is due to the fact that gp120 being associated non-covalently with gp41 becomes readily shed off the HIV particles during manipulation (35, 36), particularly during washing virus particles by centrifugation. In our experimental procedures, there were 12 steps of centrifugation of HIV-infected cells before processing for electron microscopy. Moreover, the antibody against gp120 can exert an additional tension on gp120 leading to the shedding of gp120-antibody complexes from the part of HIV virions not trapped with components of the plasma membrane. The presence of nucleolin at the external side of the plasma membrane,

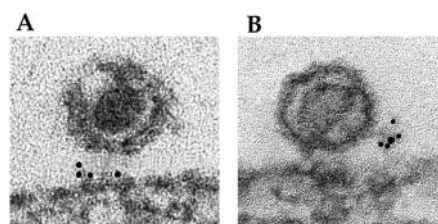


FIG. 2. Interaction of HIV particles with surface nucleolin. HIV particles bound on the surface on MT4 cells were cross-linked with an anti-HIV antibody and incubated under different conditions as described under “Experimental Procedures.” A, nucleolin was revealed by using anti-nucleolin antibodies and secondary antibodies coupled to gold beads of 10 nm. Typical results are presented here. Indeed, each time an HIV particle was observed in the close vicinity of the plasma membrane, we also detected the nucleolin signal. Note the presence of nucleolin at the external side of the plasma membrane where fiber tracts between the HIV particle and plasma membrane are observed. B, nucleolin was revealed as above, and anti-HIV antibodies were revealed by secondary antibodies coupled to gold beads of 15 nm. Four 10 nm beads corresponding to the nucleolin signal surround the 15 nm bead corresponding to the gp120 signal. As nucleolin is not detectable in concentrated HIV preparations, the 10 nm gold beads in B should correspond to surface nucleolin which looks somehow detached from the cell surface and most probably occurred during the preparation of the sample.

where fiber tracts between the HIV particle and plasma membrane are observed (37), further illustrates the colocalization of HIV particles with surface nucleolin and suggests the existence of a direct contact of HIV particles with nucleolin.

The Binding of HB-19A to the Cell-surface-expressed Nucleolin Does Not Require Heparan and Chondroitin Sulfate Proteoglycans—The specific and nonspecific binding of HB-19A to HeLa P4 cell monolayers can be monitored by washing cells at 300 and 150 mM NaCl, respectively. In cells washed at 300 mM NaCl, specific binding occurs in a dose-dependent manner and reaches a saturation at 1 μ M HB-19A (Fig. 3A), at a dose that has been shown to inhibit more than 95% HIV infection in different types of cells (1, 10). Interestingly, the nonspecific binding mostly occurred when the specific binding of HB-19A had reached saturation. Indeed, at concentrations of HB-19A less than 1 μ M there was no apparent difference between the binding values in the absence or presence of 300 mM NaCl wash.

To evaluate the potential requirement of heparan and chondroitin sulfate proteoglycans in the capacity of HB-19A to bind cells, we used Chinese hamster ovary mutant cell lines that are deficient in the expression of heparan sulfate proteoglycans (CHO 677) or both heparan and chondroitin sulfate proteoglycans (CHO 618) (28, 29). The HB-19A binding profile on the wild type CHO cells (CHO K1) was similar to that observed for the HeLa cells, because the binding was dose-dependent and reached a saturation at 1 μ M of HB-19A (Fig. 3B). Interestingly, no significant difference was observed in the HB-19A binding profile between the CHO K1 and CHO 618 that was devoid of heparan and chondroitin sulfate proteoglycans (Fig. 3B). Moreover, no significant difference was observed in the kinetics of HB-19A binding to the wild type and mutant CHO cell lines (not shown). To demonstrate that the binding of HB-19A to nucleolin is independent of heparan and chondroitin sulfate proteoglycans, we monitored the capacity of HB-19A to form a complex with the surface nucleolin expressed in different types of CHO cell lines. For this purpose, cells were incubated with the biotinylated HB-19A at 6 °C, and the complex formed between surface nucleolin and HB-19A was recovered by purification of nucleus-free extracts using avidin-agarose. The presence of nucleolin was then revealed by immunoblotting. Fig. 4 shows the recovery of surface nucleolin at comparable levels from the different CHO cell lines independent of the expression

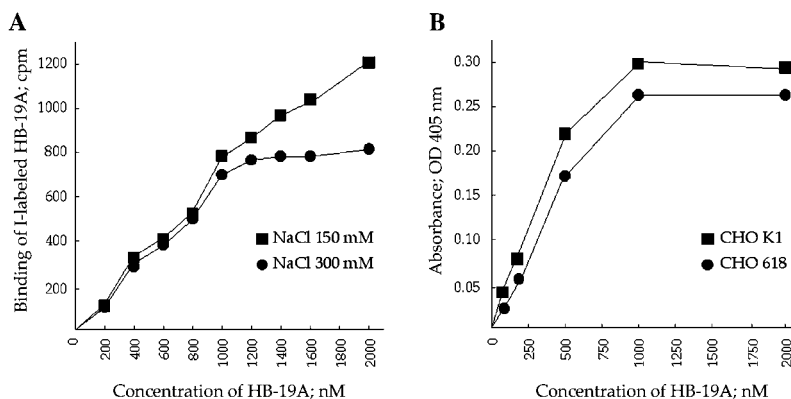


FIG. 3. **Binding of HB-19A to cells does not require heparan and chondroitin sulfate proteoglycans.** A, specific and nonspecific binding of HB-19A to cells was investigated by incubation of HeLa P4 cells with different concentrations of the ^{125}I -labeled HB-19A. The specific binding was measured after washing cells in 300 mM NaCl. B, specific binding of the biotinylated HB-19A to wild type CHO K1 cells and mutant CHO 618 cells not expressing heparan and chondroitin sulfate proteoglycans. The experimental conditions were as described under "Experimental Procedures."

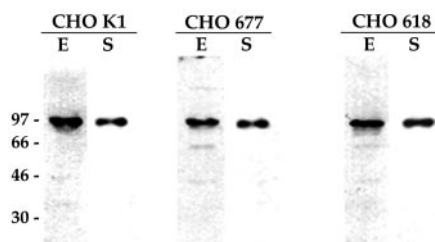


FIG. 4. **Binding of HB-19A to the cell-surface-expressed nucleolin does not require heparan and chondroitin sulfate proteoglycans.** Wild type CHO K1 cells and mutant CHO cell line 677 (not expressing heparan sulfate proteoglycans) and 618 (not expressing both heparan and chondroitin sulfate proteoglycans) were incubated with the biotinylated HB-19A for the recovery of surface-expressed nucleolin ("Experimental Procedures"). Samples of crude nucleus-free extracts (lanes E) and surface nucleolin (lanes S) were analyzed by immunoblotting for the detection of nucleolin. Material extracted from 1.5×10^6 and 10^7 cells was analyzed in lanes E and S, respectively.

of heparan and chondroitin sulfate proteoglycans. These observations are consistent with our previous results (4) showing that HB-19A binding to cells and complex formation with surface nucleolin is independent of heparan sulfate proteoglycans. In the different CHO cell clones, the amount of cell-surface nucleolin was estimated to be less than 15% of the total nucleolin recovered in the nucleus-free cell extracts.

The C-terminal Tail of Nucleolin Containing the RGG Repeats Is the Site of Binding to HB-19A—Because of the cationic nature of HB-19 analogues, we had previously proposed that the N-terminal part of nucleolin containing long stretches of acidic amino acids represents a potential binding site for these pseudopeptides (3). To illustrate this, we generated truncated constructs of nucleolin corresponding to its N- and C-terminal parts by *in vitro* transcription/translation in the rabbit reticulocyte lysate system, because the full-length nucleolin and the N-terminal part of nucleolin cannot be expressed in *E. coli* (38). In the reticulocyte lysate system, we produced [^{35}S]Met/Cys-labeled full-length nucleolin, N-terminal and the C-terminal parts containing amino acids 1–707, 1–308, and 309–707, respectively (Figs. 5A and 6). Crude labeled products were then incubated with different concentrations of the biotinylated HB-19A, and the complex was recovered by avidin-agarose. As expected, the full-length nucleolin was found to bind HB-19A. Intriguingly, the N-terminal part of nucleolin containing the acidic stretches did not bind at all, whereas the C-terminal part was bound efficiently to HB-19A (Fig. 6). To further characterize the binding domain of HB-19A, we generated truncated constructs of the C-terminal part of nucleolin in *E. coli* fused

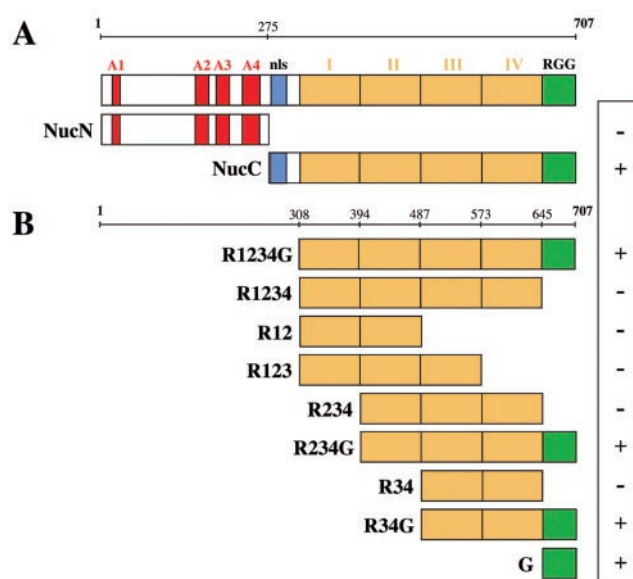


FIG. 5. **The structure of human nucleolin and deletion constructs.** A, schematic structure of nucleolin and the constructs corresponding to the N- and C-terminal parts of nucleolin. In the nucleolin structure, the positions of the long stretches of acidic domains (A1, A2, A3, and A4), the bi-partite nuclear localization signal (nls), the four RNA binding domains I, II, III, and IV, and the C-terminal tail containing the nine repeats of RGG are as indicated. The N-terminal part of nucleolin (referred to as NucN) and the C-terminal part of nucleolin (referred to as NucC) corresponded to amino acids 1–275 and 276–707, respectively. B, deletion constructs of the C-terminal part of nucleolin (amino acids 308–707). All these constructs were generated as a fusion protein with GST; GST is at the N-terminal end of the fusion protein. The C-terminal part of nucleolin was referred to as R1234G for the RNA binding domains (RBDs) I–IV and the RGG domain at the C-terminal tail. Eight deletion constructs of R1234G were generated expressing different RBDs with or without the RGG domain: R1234, R12, R123, R234, R234G, R34, R34G, and G. The – and + signs next to each construct indicates binding capacity to HB-19A.

with GST as a tag to permit their detection by antibodies against GST. The C-terminal part of nucleolin was referred to as R1234G; R1234 for the RNA binding domains (RBDs) I, II, III, and IV, and G for the RGG domain at the C-terminal tail. Eight deletion constructs of R1234G were generated expressing different RBDs with or without the RGG domain: R1234, R12, R123, R234, R234G, R34, R34G, G (Fig. 5B). The HB-19A binding capacity of each construct was then investigated by incubation of crude bacterial extracts with the biotinylated HB-19A. The results show that the presence of the RGG do-

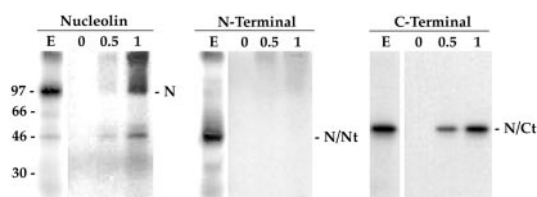


FIG. 6. **HB-19A binds to the C-terminal part of nucleolin.** The [³⁵S]Met/Cys-labeled full-length nucleolin, N-terminal and the C-terminal parts containing amino acids 1–707, 1–275, and 276–707, respectively, were generated using an *in vitro* transcription-translation system. Crude labeled products were then incubated with 0, 0.5, or 1 μ M biotinylated HB-19A, and the complexes formed between nucleolin and HB-19A were recovered by avidin-agarose (lanes 0, 0.5, and 1). The purified proteins were eluted by heating in the electrophoresis sample buffer containing SDS, analyzed by SDS-PAGE, and the labeled bands revealed by fluorography (“Experimental Procedures”). An aliquot of the crude labeled products was diluted in an equal volume of 2 \times electrophoresis sample buffer containing SDS and analyzed by SDS-PAGE (lanes E). N, N/Nt, and N/Ct indicate the position of the full-length nucleolin, nucleolin/N-terminal part, and nucleolin/C-terminal part, respectively. The numbers on the left indicate the position of molecular mass (in kDa) protein markers.

main determines the HB-19A binding capacity of a given construct in the C-terminal part of nucleolin. Furthermore, the RGG domain alone is sufficient for binding (Fig. 7). The faint binding of some constructs lacking the RGG domain was most probably nonspecific because it was not dependent on the concentration of HB-19A (Fig. 8, lanes R1234 and R234). On the other hand, the binding of constructs containing the RGG domain was increased with the dose of HB-19A and reached a maximum value at 5 μ M HB-19A (Fig. 8, lanes 1234G, R234G, and G).

The C-terminal Part of Nucleolin Containing the RGG Domain Inhibits HIV Infection—The nucleolin constructs R1234G and R1234 were purified by using a glutathione-Sepharose column and assayed for their potential capacity to inhibit HIV-1 infection in the HeLa P4 cell experimental model (Fig. 9). The HeLa P4 cells provide an efficient system to monitor inhibitors of the T-lymphocyte-tropic HIV-1 LAI attachment and entry into cells. For example, pretreatment of cells with HB-19 or HB-19A leads to inhibition of HIV entry at the level of HIV attachment to cells (1, 4) (Fig. 9). In the presence of the R1234G construct, HIV infection was inhibited by more than 75%, whereas the R1234 construct lacking the RGG domain had no effect. In view of this result, we then synthesized a peptide corresponding to the last 63 amino acids of nucleolin containing the nine repeats of RGG. This peptide referred to as NP63, for nucleolin peptide containing 63 amino acids, inhibited completely HIV-1 LAI infection (Fig. 9A). The NP63 effect was most probably mediated via its affinity to bind HIV. Indeed, cells pretreated with NP63 manifested no resistance to HIV when the culture supernatants containing the peptide were replaced by fresh culture media before addition of HIV (not shown). In contrast, we have demonstrated previously (1) that HB-19-pretreated cells remain resistant to HIV even several hours after removal of the culture medium containing the inhibitor. NP63 inhibited HIV-1 LAI infection in a dose-dependent manner with an IC_{50} value of 5 μ M (Fig. 9B). This was the consequence of inhibition of virus attachment to cells in a dose-dependent manner (Fig. 9D). The IC_{50} value for the inhibition of HIV-1 LAI attachment by NP63 was estimated to be 5 μ M. The inhibitory effect of N63 was not restricted to T-lymphocyte-tropic HIV-1 isolates, because it inhibited also macrophage-tropic HIV-1 Ba-L isolate in a dose-dependent manner with an IC_{50} value of 1 μ M (Fig. 9C). Therefore, HIV-1 Ba-L appears to be more sensitive to the inhibitory effect of N63 compared with HIV-1 LAI. Whether this is due to the presence

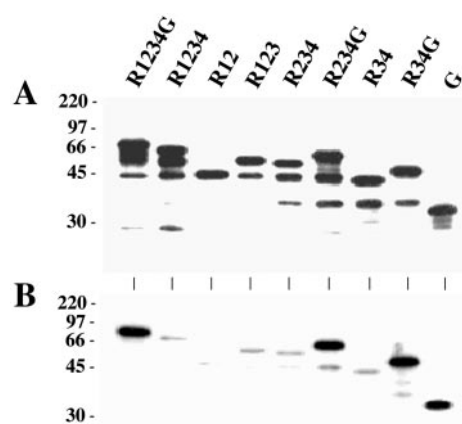


FIG. 7. **HB-19A binds the RGG domain in the C-terminal part of nucleolin.** A, expression of the GST fusion/deletion constructs of the C-terminal part of nucleolin. Aliquots of the crude bacterial extracts (containing equivalent amounts of protein) were diluted in an equal volume of 2 \times electrophoresis sample buffer containing SDS and analyzed by immunoblotting using anti-GST antibodies. In the different constructs, the bands lower than the most upper band represent degradation products. (Partial cleavage of nucleolin has been shown to occur under different experimental conditions (3, 52).) B, the binding of the constructs to HB-19A. Aliquots of the crude bacterial extracts (containing equivalent amounts of protein) were incubated with 5 μ M of the biotinylated HB-19A, and the complexes formed between a given construct and HB-19A were recovered by avidin-agarose. The purified proteins were eluted by heating in the electrophoresis sample buffer containing SDS and analyzed by immunoblotting using anti-GST antibodies. Experimental details are described under “Experimental Procedures.” The numbers on the left (in A and B) indicate the position of molecular mass (in kDa) protein markers.

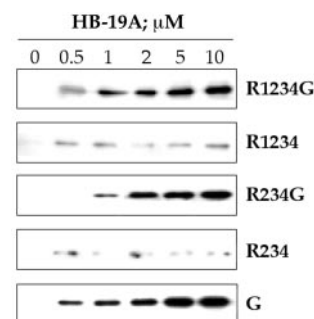


FIG. 8. **The dose-dependent binding of HB-19A to the C-terminal part of nucleolin.** Aliquots of the crude bacterial extracts (containing equivalent amounts of protein) were incubated with the biotinylated HB-19A at 0, 0.5, 1, 2, 5, and 10 μ M concentrations, and the complexes formed between a given construct and HB-19A were recovered by avidin-agarose. The purified proteins were eluted by heating in the electrophoresis sample buffer containing SDS, analyzed by immunoblotting using anti-GST antibodies. A section of each gel in the region of the corresponding band is presented.

of a lower number of basic residues in the V3 loop of macrophage-tropic HIV-1 isolates compared with that of T-lymphocyte-tropic HIV-1 isolates (39) remains to be investigated.

DISCUSSION

We have reported previously (4) that HIV particles can prevent the binding of HB-19 to cells and complex formation with surface nucleolin, thus suggesting that HB-19 and HIV interact with a common site in nucleolin. Accordingly, cross-linking of either cell-bound HB-19A or HIV particles leads to capping of surface nucleolin in accord with ligand-dependent clustering of a common surface receptor. These observations and the presence of surface nucleolin in the vicinity of HIV particles observed in electron micrographs are consistent with the implication of surface nucleolin in the HIV attachment and

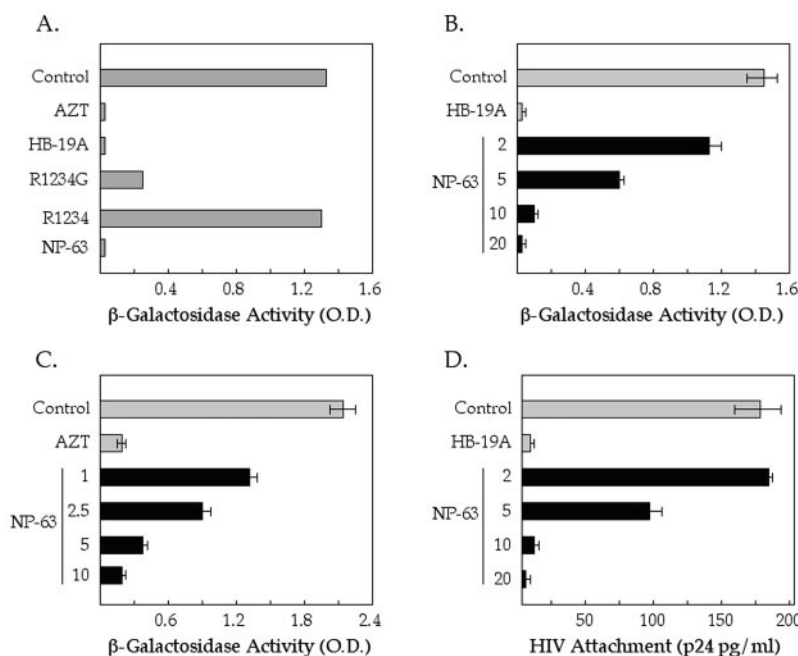


FIG. 9. The RGG domain of nucleolin inhibits HIV infection by blocking attachment of virus particles to cells. A, inhibition of HIV infection by the C-terminal part of nucleolin. HIV-1 LAI infection was monitored in HeLa P4 cells by the expression of the *lacZ* gene (corresponding to β -galactosidase) under the control of HIV-1 LTR (1). Cells were infected in the presence of either AZT (5 μ M), HB-19A (1 μ M), R1234G and R1234 constructs (each at 25 μ g/ml), and NP63 peptide (20 μ M). The β -galactosidase activity was measured at 48 h post-infection ($A_{570\text{ nm}}$). Each point represents the mean of duplicate samples. B, the NP-63 peptide corresponding to the RGG domain of nucleolin inhibits HIV-1 LAI infection in a dose-dependent manner. HeLa P4 cells were infected in the presence of HB-19A (1 μ M) or 2, 5, 10, and 20 μ M of the NP63 peptide. The β -galactosidase activity was measured as in A. The mean \pm S.D. of triplicate samples is shown. C, the NP-63 peptide inhibits HIV-1 LAI infection in HeLa P4-C5 cells in a dose-dependent manner. HeLa P4-C5 cells were infected in the presence of AZT (5 μ M) or 1, 2.5, 5, and 10 μ M of the NP63 peptide. The β -galactosidase activity was measured as in A. The mean \pm S.D. of triplicate samples is shown. Note that at 10 μ M of the NP63 peptide the inhibition is as efficient as AZT (which gives the background value in HeLa P4-C5 cells). D, the NP-63 peptide corresponding to the RGG domain of nucleolin inhibits HIV attachment. Assay of HIV-1 LAI attachment ("Experimental Procedures") was performed in the presence of HB-19A (1 μ M) or 2, 5, 10, and 20 μ M of the NP63 peptide. The concentration of the HIV-1 core protein p24 was measured in cell extracts as an estimation of the amount of HIV attached to cells. The mean \pm S.D. of triplicate samples is shown.

anchorage process. By the *in vitro* transcription-translation system, we identified that the C-terminal part of nucleolin is the domain that binds HB-19A, whereas the N-terminal part does not bind at all. This lack of interaction between the cationic HB-19A and the N-terminal part of nucleolin containing long stretches of acidic amino acid residues, and its specific binding to cells independent of expression of anionic proteoglycans, indicates that the binding of HB-19A with nucleolin is not simply a matter of charge. The specific nature of HB-19 interaction with nucleolin has also been demonstrated recently *in vivo* in rats (33). Indeed, HB-19 was shown to be preferentially taken up *in vivo* by lymphoid organs where it forms a stable complex with nucleolin. Thus the molecular target of HB-19 *in vivo* is once again nucleolin (33).

Several reports (3, 4, 15, 18, 19, 21, 22) have demonstrated that surface nucleolin functions as a receptor for different ligands. By studies using electron and confocal laser immunofluorescence microscopy, we have confirmed that nucleolin is expressed at the cell surface where it exists in close association with the intracellular actin cytoskeleton (20). As the amino acid sequence of nucleolin does not predict a hydrophobic domain to account for its anchorage into the plasma membrane, association of nucleolin with actin could be mediated by an integral membrane protein that binds both nucleolin and actin filaments. Whatever is the case, surface nucleolin is tightly associated with the plasma membrane because extensive washing of cells with high concentrations of EDTA, EGTA, or NaCl has no effect (20). However, surface nucleolin is readily solubilized by treatment of cells with a non-ionic detergent. Recently, we reported that surface nucleolin becomes detergent-resistant

following HIV anchorage to cells and is recovered along detergent-insoluble membrane microdomains containing lipid raft components, such as CD59 and CD90 (34). At the cell surface, cross-linking of HIV particles results in coaggregation of HIV particles with CD4, CXCR4, CD56, and CD90 in addition to surface nucleolin. The aggregation of these antigens is a specific event because the surface distribution and organization CD45 are not affected. Equilibrium density fractionation of extracts from infected cells revealed that HIV proteins and nucleolin copurify with Triton X-100-resistant glycolipid-enriched membrane microdomains-associated proteins. After HIV entry, nucleolin is recovered also in fractions containing HIV DNA, viral matrix, and reverse transcriptase, thus suggesting that it could accompany viral entry. Interestingly, surface nucleolin is markedly down-regulated a few hours following HIV entry into permissive cells, an effect that appears to be the consequence of its translocation into the cytoplasm. Thus anchorage of HIV particles on permissive cells induces aggregation of surface nucleolin and its association with detergent-insoluble lipid raft components. Moreover, our results also supported the suggestion that surface nucleolin and lipid rafts are implicated in early events in the HIV entry process (34).

By using truncated deletion constructs of the C-terminal part of nucleolin, we identified the C-terminal tail of nucleolin containing the RGG domain as the site that binds the pseudopeptide HB-19A. Preliminary observations suggest that the nine RGG repeats at the C-terminal tail of nucleolin are necessary for HB-19A binding. Indeed, synthetic peptides containing four or five RGG repeats were found not to bind HB-19A and moreover not affect HIV infection (data not shown). Consequently, the nine RGG repeats in the nucleolin tail appear to

be required to generate a conformation that is optimum for HB-19A binding and inhibition of HIV infection. The arginine residues in the RGG domain of nucleolin purified from eucaryotic cells are found to exist as N^G, N^G -dimethylarginine (40, 41). The significance of this post-translational modification of the RGG domain on the binding to HB-19A is not known. However, it is unlikely that it is essential for HB-19A binding because the nucleolin C-terminal constructs expressing the RGG domain that we generated in *E. coli* were shown to bind HB-19A efficiently. Previously, the RGG domain in nucleolin has been reported to bind RNA (42), rDNA (43), and subset of ribosomal proteins (44). Studies using a combination of circular dichroism and infrared spectroscopy have provided evidence that repeated β -turns are a major structural component of the RGG domain and might play a role in the formation of protein-protein interactions (42). It should also be noted that the RGG domain contains five phenylalanine residues that potentially could establish cation- π interactions (45) with the arginine and lysine residues accessible in HB-19A or in the V3 loop of HIV. Indeed, a large amount of evidence has now established the importance of the cation- π interactions as a force for molecular recognition in a number of biological binding sites for cations. The cation- π interaction is a general noncovalent binding force, in which the face of an aromatic ring (Phe, Tyr, and Trp) provides a region of negative electrostatic potential that can bind cations with considerable strength (45, 46). The cation- π interactions have been considered in such diverse systems as acetylcholine receptors, K^+ channels, the cyclase methylation reactions involving *S*-adenosylmethionine, and finally in specific drug-receptor interactions (45, 47, 48). Recently, cation- π interactions between amino acid side chains of basic amino residues on the one hand and of the aromatic amino acids on other hand have been shown to play an important role in intermolecular recognition at the protein-protein interface (49). In accord with this, the RGG domain has been implicated in the process of self-annealing of nucleolin (50). Interestingly, an analogous RGG domain in the C terminus of the heterogeneous nuclear ribonucleoprotein A1 has also been shown to mediate protein-protein interactions (51). As the RGG domain in nucleolin is the binding site of HB-19A, then the C-terminal tail of nucleolin should be well exposed on the cell surface because HB-19 and HB-19A analogues bind readily to the cell-surface-expressed nucleolin (4) (Fig. 4). We have reported (3) that the HIV-1 external envelope gp120 binds with high affinity a partially purified preparation of nucleolin. The fact that the binding of gp120 to nucleolin is inhibited by HB-19 suggests that the RGG domain in surface nucleolin could represent a potential site for binding of HIV particles.

The demonstration that the anti-HIV pseudopeptide binds the C-terminal RGG domain of nucleolin further demonstrates that nucleolin is a specific target for the action of inhibitors of HIV infection (1, 4). This and the fact that the synthetic NP63 peptide corresponding to the RGG domain inhibits HIV infection by preventing virus binding to cells is consistent with the implication of nucleolin at an early phase of HIV infection. As the NP63 peptide inhibits HIV attachment in a dose-dependent manner, it provides a novel inhibitor of HIV infection that blocks virus particle attachment to cells. The NP63 peptide could be used as a model for the development of novel inhibitors of HIV infection with a distinct mode of antiviral action.

Acknowledgments—We thank Josette Svab and Nadine Robert for excellent technical assistance and Emmanuelle Perret for confocal microscopy.

REFERENCES

- Nisole, S., Krust, B., Dam, E., Bianco, A., Seddiki, N., Loac, S., Callebaut, C., Guichard, G., Muller, S., Briand, J. P., and Hovanessian, A. G. (2000) *AIDS Res. Hum. Retroviruses* **16**, 237–249
- Ugolini, S., Mondor, I., and Sattentau, Q. J. (1999) *Trends Microbiol.* **7**, 144–149
- Callebaut, C., Blanco, J., Benkirane, N., Krust, B., Jacotot, E., Guichard, G., Seddiki, N., Svab, J., Dam, E., Muller, S., Briand, J. P., and Hovanessian, A. G. (1998) *J. Biol. Chem.* **273**, 21988–21997
- Nisole, S., Krust, B., Callebaut, C., Guichard, G., Muller, S., Briand, J. P., and Hovanessian, A. G. (1999) *J. Biol. Chem.* **274**, 27875–27884
- Valenzuela, A., Blanco, J., Krust, B., Franco, R., and Hovanessian, A. G. (1997) *J. Virol.* **71**, 8289–8298
- Roderiquez, G., Oravec, T., Yanagishita, M., Chequer Bou-Habib, D., Mostowski, H., and Norcross, M. A. (1995) *J. Virol.* **69**, 2233–2239
- Mondor, I., Ugolini, S., and Sattentau, Q. J. (1998) *J. Virol.* **72**, 3623–3634
- Saphire, A. C. S., Bobardt, M. D., and Gallay, P. A. (1999) *EMBO J.* **18**, 6771–6785
- Moulard, M., Lortat-Jacob, H., Mondor, I., Roca, G., Wyatt, R., Sodroski, J., Zhao, L., Olson, W., Kwong, P. D., and Sattentau, Q. J. (2000) *J. Virol.* **74**, 1948–1960
- Callebaut, C., Jacotot, E., Guichard, G., Krust, B., Rey-Cuille, M. A., Cointe, D., Benkirane, N., Blanco, J., Muller, S., Briand, J. P., and Hovanessian, A. G. (1996) *Virology* **218**, 181–192
- Seddiki, N., Nisole, S., Krust, B., Callebaut, C., Guichard, G., Muller, S., Briand, J. P., and Hovanessian, A. G. (1999) *AIDS Res. Hum. Retroviruses* **15**, 381–390
- Callebaut, C., Jacotot, E., Krust, B., Guichard, G., Blanco, J., Svab, J., Muller, S., Briand, J. P., and Hovanessian, A. G. (1997) *J. Biol. Chem.* **272**, 7159–7166
- Callebaut, C., Nisole, S., Briand, J. P., Krust, B., and Hovanessian, A. G. (2001) *Virology* **281**, 248–264
- Ginisty, H., Sicard, H., Roger, B., and Bouvet, P. (1999) *J. Cell Sci.* **112**, 761–772
- Srivastava, M., and Pollard, H. B. (1999) *FASEB J.* **13**, 1911–1922
- Sememkovich, C. F., Ostlund, R. E., Olson, M. O., and Yang, J. W. (1990) *Biochemistry* **29**, 9708–9713
- Kleinman, H. K., Weeks, B. S., Cannon, F. B., Sweeney, T. M., Sephel, G. C., Clement, B., Zain, M., Olson, M. O. J., Jucker, M., and Burrous, B. A. (1991) *Arch. Biochem. Biophys.* **290**, 320–325
- Krantz, S., Salazar, R., Brandt, R., Kellerman, J., and Lottspeich, F. (1995) *Biochim. Biophys. Acta* **1266**, 109–112
- De Verdugo, U. R., Selinkgra, H. C., Huber, M., Kramer, B., Kellermann, J., Hofschneider, P. H., and Kandolf, R. (1995) *J. Virol.* **69**, 6751–6757
- Hovanessian, A. G., Puvion-Dutilleul, F., Nisole, S., Svab, J., Perret, E., Deng, J. S., and Krust, B. (2000) *Exp. Cell Res.* **261**, 312–328
- Dumler, I., Stepanova, V., Jerke, U., Mayboroda, O. A., Vogel, F., Bouvet, P., Thachuk, V., Haller, H., and Gulba, D. C. (1999) *Curr. Biol.* **9**, 1468–1476
- Larrucea, S., Cambrono, R., Gonzalez-Rubio, C., Fraile, B., Gamallo, C., Fontan, G., and Lopez-Trascasa, M. (1999) *Biochem. Biophys. Res. Commun.* **266**, 51–57
- Srivastava, M., Fleming, P. J., Pollard, H. B., and Burns, A. L. (1989) *FEBS Lett.* **250**, 99–105
- Deng, J.-S., Baillou, B., and Hofmeister, J. K. (1996) *Mol. Biol. Rep.* **23**, 191–195
- Murakami, T., Nakajima, T., Koyanagi, Y., Tachibana, K., Fujii, N., Tamamura, H., Yoshida, N., Waki, M., Matsumoto, A., Yoshie, O., Kishimoto, T., Yamamoto, N., and Nagasawa, T. (1997) *J. Exp. Med.* **186**, 1389–1393
- Tamamura, H., Waki, M., Imai, M., Otaka, A., Ibusa, T., Waki, K., Miyamoto, K., Matsumoto, A., Murakami, T., Nakashima, H., Yamamoto, N., and Fujii, N. (1998) *Bioorg. Med. Chem.* **6**, 473–479
- Limal, D., Briand, J.-P., Dalbon, P., and Joliver, M. (1998) *J. Peptide Res.* **52**, 121–129
- Esko, J. D., Weinke, J. L., Taylor, W. H., Ekborg, G., Rodén, L., Anantharamaiah, G., and Gawish, A. (1987) *J. Biol. Chem.* **262**, 12189–12195
- Esko, J. D., Rostand, K. S., and Weinke, J. L. (1988) *Science* **241**, 1092–1096
- Gartner, S., Markovits, P., Markovitz, D. M., Kaplan, M. H., Gallo, R. C., and Popovic, M. (1986) *Science* **233**, 215–219
- Krust, B., Callebaut, C., and Hovanessian, A. G. (1993) *AIDS Res. Hum. Retroviruses* **9**, 1087–1090
- Maréchal, V., Clavel, F., Heard, J.-M., and Schwartz, O. (1998) *J. Virol.* **72**, 2208–2212
- Krust, B., Vignet, R., Cardona, A., Rougeot, C., Jacotot, E., Callebaut, C., Guichard, G., Briand, J. P., Grognet, J. M., Hovanessian, A. G., and Edelman, L. (2001) *Proc. Natl. Acad. Sci. U. S. A.* **98**, 14090–14095
- Nisole, S., Krust, B., and Hovanessian, A. G. (2002) *Exp. Cell Res.*, in press
- Schneider, J., Kaaden, O., Copeland, T. D., Oroszlan, S., and Hunsmann, G. (1986) *J. Gen. Virol.* **67**, 2533–2538
- Wyatt, R., Kwong, P. D., Desjardins, E., Sweet, R. W., Robinson, J., Hendrickson, W. A., and Sodroski, J. G. (1998) *Nature* **393**, 705–711
- Staubler, R. H., Rulong, S., Palm, G., and Tarasova, N. I. (1999) *Biochem. Biophys. Res. Commun.* **258**, 695–702
- Hanakahi, L. A., Dempsey, L. A., Li, M.-J., and Maizels, N. (1997) *Proc. Natl. Acad. Sci. U. S. A.* **94**, 3605–3610
- De Jong, J.-J., De Ronde, A., Keulen, W., Tersmette, M., and Goudsmit, J. (1992) *J. Virol.* **66**, 6777–6780
- Lischwe, M. A., Cook, R. G., Ahn, Y. S., Yeoman, L. C., and Busch, H. (1985) *Am. Chem. Soc.* **24**, 6025–6028
- Lapeyre, B., Amalric, F., Ghaffari, S. H., Venkatarama Rao, S. V., Dumbar, T. S., and Olson, M. O. J. (1986) *J. Biol. Chem.* **261**, 9167–9173
- Ghisolfi, L., Joseph, G., Amalric, F., and Erard, M. (1992) *J. Biol. Chem.* **267**, 2955–2959

43. Hanakahi, L. A., Sun, H., and Maizels, N. (1999) *J. Biol. Chem.* **274**, 15908–15912
44. Bouvet, P., Diaz, J.-J., Kindbeiter, K., Madjar, J.-J., and Amalric, F. (1998) *J. Biol. Chem.* **273**, 1902–19029
45. Dougherty, D. A. (1996) *Science* **271**, 163–168
46. Gallivan, J. P., and Dougherty, D. A. (1999) *Proc. Natl. Acad. Sci. U. S. A.* **96**, 9459–9464
47. Mecozzi, S., West, A. P., and Dougherty, D. A. (1996) *Proc. Natl. Acad. Sci. U. S. A.* **93**, 10566–10571
48. Zhong, W., Gallivan, J. P., Zhang, Y., Li, L., Lester, H. A., and Dougherty, D. A. (1998) *Proc. Natl. Acad. Sci. U. S. A.* **95**, 12088–12093
49. Pletneva, E. V., Laederach, A. T., Fulton, D. B., and Kostić, N. M. (2001) *J. Am. Chem. Soc.* **123**, 6232–6245
50. Hanakahi, L. A., Bu, Z., and Maizels, N. (2000) *Biochem. Biophys. Res. Commun.* **39**, 15493–15499
51. Cartegni, L., Maconi, M., Morandi, E., Cobianchi, F., Riva, S., and Biamonti, G. (1996) *J. Mol. Biol.* **259**, 337–348
52. Fang, S.-H., and Yeh, N.-H. (1993) *Exp. Cell Res.* **208**, 48–53

The Anti-HIV Pentameric Pseudopeptide HB-19 Binds the C-terminal End of Nucleolin and Prevents Anchorage of Virus Particles in the Plasma Membrane of Target Cells

Sébastien Nisole, Elias A. Said, Claudia Mische, Marie-Christine Prevost, Bernard Krust, Philippe Bouvet, Alberto Bianco, Jean-Paul Briand and Ara G. Hovanessian

J. Biol. Chem. 2002, 277:20877-20886.

doi: 10.1074/jbc.M110024200 originally published online March 27, 2002

Access the most updated version of this article at doi: [10.1074/jbc.M110024200](https://doi.org/10.1074/jbc.M110024200)

Alerts:

- [When this article is cited](#)
- [When a correction for this article is posted](#)

[Click here](#) to choose from all of JBC's e-mail alerts

This article cites 51 references, 26 of which can be accessed free at <http://www.jbc.org/content/277/23/20877.full.html#ref-list-1>